J. Phys. Chem. B **2007,** *111,* 4271−4279

Peptide Bond Vibrational Coupling

Nataliya S. Myshakina and Sanford A. Asher*

Department of Chemistry, University of Pittsburgh, Pittsburgh, Pennsylvania 15260

Received: August 14, 2006; In Final Form: January 3, 2007

Neutral trialanine (Ala_3), which is geometrically constrained to have its peptide bond at Φ and Ψ angles of α-helix and PPII-like conformers, are studied at the B3LYP/6-31+G(d,p) level of theory to examine vibrational interactions between adjacent peptide units. Delocalization of the amide I, amide II, and amide III_3 vibrations are analyzed by calculating their potential energy distributions (PED). The vibrational coupling strengths are estimated from the frequency shifts between the amide vibrations of Ala_3 and the local amide bond vibrations of isotopically substituted Ala_3 derivatives. Our calculations show the absence of vibrational coupling of the amide I and amide II bands in the PPII conformations. In contrast, the α-helical conformation shows strong coupling between the amide I vibrations due to the favorable orientation of the C=O bonds and the strong transitional dipole coupling. The amide III_3 vibration shows weak coupling in both the α-helix and PPII conformations; this band can be treated as a local independent vibration. Our calculated results in general agree with our previous experimental UV Raman studies of a 21-residue mainly alanine-based peptide (AP).

Introduction

Vibrational spectroscopy is a powerful method for determining molecular structure and dynamics, as evident from the numerous IR and Raman studies that have examined the conformations and dynamics of peptides and proteins.[1−15] These studies interpret spectral changes in terms of alterations in equilibrium conformations. Most often, the underlying assumption is that the systems are linear and that the measured spectra derive from a weighted linear sum of the spectral contributions of the individual conformations. In the case of peptide secondary structure studies, it is assumed that the spectra are the linear sum of the spectra of the individual peptide bonds and that the individual peptide bond spectra are uniquely characteristic of the conformation about each peptide bond. This presumption assumes that there is negligible coupling between the atomic motions of adjacent peptide bonds.

If significant coupling occurs between adjacent peptide bonds, the individual peptide bond spectra would depend upon their context. In this case, a simple linear interpretation of the resultant observed spectra becomes impossible. It would, thus, become necessary to understand the dependence of the peptide bond spectra on coupling of atomic motions between adjacent peptide bonds. This coupling can be studied theoretically by calculating the normal modes of peptides.

Previous studies, which have examined vibrational coupling between the same peptide bond vibrations between peptide bond units, have mainly focused on the amide I vibration, which is primarily a C=O stretching mode mixed with minor contributions from C−N stretching and C_α−C−N deformation.[2,4,5,16−27] It has been demonstrated that the amide I vibrations of polypeptides show significant coupling and are delocalized across many peptide bonds. The coupling between the amide I vibrations is enabled by its large transition dipole moment as shown by Krimm and co-workers.[28−31]

Very few studies have examined vibrational coupling between the amide II (C−N stretching and N−H bending coupled out-of-phase) vibrations of adjacent peptide units and the coupling between amide III vibrations (C−N stretching and N−H bending coupled in-phase) of adjacent peptide units.[32] These couplings should be smaller than that of the amide I vibrations because the transition dipoles are smaller. Understanding the extent of coupling of the amide III vibrations is important because the amide III Raman bands are the most sensitive to peptide conformation. In fact, the lowest frequency amide III band component, which is denoted as the amide III_3 vibration, is a sensitive probe of the peptide bond Ψ angle.[33−35] It is important to understand whether the amide III_3 vibration is a local mode or if it involves collective peptide unit motion; is its frequency determined solely by the conformation of the vibrating peptide unit, or is its frequency also determined by the conformation of adjacent peptide units?

To examine the extent of coupling of amide I, amide II, and amide III_3 vibrations between peptide units, we previously experimentally studied this coupling by examining the UV resonance Raman spectra (UVRS) of two linked amides in mixed H_2O/D_2O solutions.[36] We also examined the 21-residue mainly poly Ala peptide (AP), which is ~50% α-helix at 0 °C and melts to a polyproline II (PPII) conformation at higher temperatures.[36,37] Our hypothesis was that if the peptide vibrations were coupled, then partial deuteration of the amide nitrogens would alter the amide bond vibrations dramatically, because deuteration of the N−H decouples N−H bending from C−N stretching. This large mass change would dramatically change the specific peptide bond amide vibrations. Thus, the partially deuterated spectrum would not simply be the sum of the spectra of the fully deuterated and non-deuterated peptides.

These studies[36,37] suggested essential vibrational independence of the amide III_3 and amide II bands for linked peptide bonds in both the α-helix and PPII conformations of AP. In addition, the amide I and amide I′ vibrations showed no evidence for coupling in the case of the AP PPII conformation, and the amide I band of the α-helix conformation showed significant inter-peptide bond coupling.

---

* Corresponding author. E-mail: asher@pitt.edu. Telephone: (412)-624-8570. Fax: (412)-624-0588.

10.1021/jp065247i CCC: $37.00

The weakness of our experimental study was that we did not know the magnitude expected for the band frequency perturbation due to coupling of adjacent peptide bonds. In the work here, we further clarify the extent of interpeptide coupling using vibrational analysis calculated by using electronic structure methods. We examined trialanine (Ala_3) as a model peptide to study vibrational interactions between adjacent peptide units and studied the normal mode compositions of the amide I, amide II, and amide III_3 vibrations for geometries constrained to occur in the PPII and α-helical conformations.

We also calculated the normal modes for several Ala_3 isotopomers where we reduce coupling between adjacent substituents and peptide bonds by altering the atomic masses. We used these calculated local mode frequencies to estimate the magnitude of the amide band frequency shifts due to vibrational coupling.

Computational Details

All calculations were performed at the density functional theory[38−40] (DFT) level by using the Gaussian 03 calculation package.[41] Geometry optimization and vibrational frequency analysis were carried out by using B3LYP functional[42−44] and a 6-31+G(d,p) basis set. Partial geometry optimization was performed for trialanine (Ala_3) in vacuum with each specified pair of fixed values of φ and ψ angles corresponding to α-helical ($\varphi = -76°$; $\psi = -44°$) and PPII-like ($\varphi = -67°$; $\psi = 132°$) secondary structures. The values of the φ- and ψ-angles were taken from the molecular dynamics study performed by Mu et al.[45] The authors showed that conformations with these particular values of ψ and φ angles are the most populated by short peptides. To take into account frequency shifts that occur in the PPII conformation due to peptide−water hydrogen-bonding, we partially optimized the geometry and calculated frequencies for Ala_3 in a PPII conformation surrounded by water molecules.

We calculated the normal modes of Ala_3 in both the α-helical and PPII conformations for the natural abundance and the following isotopomers: $^{13}C{=}^{18}O$ substituted at the N-terminus peptide unit, $^{13}C{=}^{18}O$ substituted at the C-terminus peptide unit, N−D substituted at the N-terminus peptide unit, N−D substituted at the C-terminus peptide unit, ND_2 substituted at the N-terminus amide group, simultaneous ND_2 substitution and N−D substitution at the N-terminus peptide unit, and simultaneous ND_2 substitution and N−D substitution at the C-terminus peptide unit. The harmonic vibrational frequencies were corrected by the previously suggested scaling factor of 0.97.[46,47] We calculated the potential energy distribution (PED) by using the GAR2PED Gaussian output processing program written by J. M. L. Martin and C. Van Alsenoy.[48]

To distinguish contributions of the nuclear motions of different peptide units to the calculated normal mode composition, we labeled the internal vibrational coordinates (bonds, valence and torsion angles corresponding to stretching, bending and torsional vibrations, respectively, Figure 1).

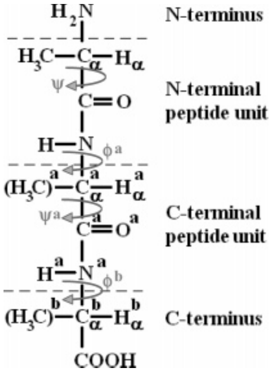

Figure 1. Labeling of peptide atoms indicating definitions of peptide unit and Ψ and ϕ angles.

Results and Discussion

Normal Mode Composition Analysis. *Amide I.* Our previous experimental study of the UVRS of the 21-residue AP peptide in pure water, pure D_2O, and H_2O/D_2O mixtures concluded that the amide I vibrations are coupled in α-helical AP and uncoupled in the PPII conformation.[37] This conclusion is consistent with the results of Hochstrasser's group.[5,24]

Our α-helical Ala_3 vibrational analysis demonstrates two amide I modes, a high frequency A symmetry vibration (1716 cm^{-1}), and a lower frequency E_1 symmetry vibration (1702 cm^{-1}) (Table 1). Each mode contains CO stretching contributions from both peptide units.

In contrast, the two amide I modes calculated for the PPII conformation of Ala_3 are essentially local vibrations of the individual CO stretches. These results agree with our experimental data, which indicated coupled amide I modes in the α-helical conformation but local amide I modes in the PPII conformation.

Amide II. In D_2O, N−H deuteration causes the complex amide II vibration to become an almost pure C−N stretch (amide II′) due to decoupling of N−H bending from C−N stretching.[49,50] The amide II′ appears as a doublet in *N*-methylacetamide (NMA) and AP because of a Fermi resonance between the amide II′ vibration and a combination of the low frequency amide IV′ (632 cm^{-1}) and a skeletal deformation vibration (∼873 cm^{-1}).[50]

Our theoretical results for the amide II of α-helical Ala_3 indicate more coupling than our experimental studies do. Experimentally, we did not observe a clear frequency shift for the amide II and amide II′ bands in the PPII and α-helix conformations of AP upon adjacent peptide bond deuteration/protonation. Unfortunately, we were unable to completely exclude small frequency shifts for the amide II bands due to

TABLE 1: Amide I Frequencies and Normal Mode Compositions of Ala_3 in α-Helix and PPII Conformations[a]

conformer	ν, cm^{-1}	PED, %
α-helix	1702	N-term PU: CO s (51), $NC_{\alpha}C$ b (4), −CN s (4), $-C_{\alpha}C$ s (2), NH inp b (1), $-CN_{p}C_{\alpha}$ b (1) C-term PU: $-C^{a}O^{a}$ s (27), $C_{\alpha}^{a}N^{a}C^{a}$ b (2), $C^{a}N^{a}$ s (2), $C_{\alpha}^{a}CN$ b (1), $C^{a}C_{\alpha}^{a}$ s (1), $-C^{a}C_{\alpha}^{b}N^{a}$ b (1)
	1716	C-term PU: $C^{a}O^{a}$ s (52), $C_{\alpha}^{a}N^{a}C^{a}$ b (4), $-C^{a}N^{a}$ s (3), $-C^{a}C_{\alpha}^{a}$ s (2), $-N^{a}H^{a}$ inp b (2), $C^{a}C_{\alpha}^{b}N^{a}$ b (1), $-C^{a}NC_{\alpha}^{a}$ b (1) N-term PU: CO s (27), $NC_{\alpha}C$ b (2), −CN s (2), $-C_{\alpha}C$ s (1), −NH inp b (1), $C_{\alpha}^{a}CN$ b (1)
PPII	1695	N-term PU: CO s (70), $NC_{\alpha}C$ b (6), −CN s (5), $-NH_2$ scs (4), $-C_{\alpha}C$ s (3), $-C^{a}O^{a}$ s (3), −NH inp b (2), $CN_{p}C_{\alpha}$ b (2), $C_{\alpha}^{a}CN$ b (2), $-CC_{\beta}C_{\alpha}$ b (1)
	1698	C-term PU: $C^{a}O^{a}$ s (75), $-C^{a}N^{a}$ s (7), $C_{\alpha}^{a}N^{a}C^{a}$ b (6), CO s (3), $-C^{a}C_{\alpha}^{a}$ s (3), $-N^{a}H^{a}$ inp b (2), $C^{a}C_{\alpha}^{b}N^{a}$ b (2), $C^{a}NC_{\alpha}^{a}$ b (1)

[a] Frequencies are scaled by factor 0.97. Abbreviations: PU, peptide unit; s, stretch; b, bending; inp b, in-plane bending; scs, scissoring.

TABLE 2: Calculated Amide II Frequencies and Normal Mode Compositions (PED) for Ala_3 in α-Helical and PPII Conformations[a]

conformer	ν, cm^{-1}	PED, %
α-helix	1480	N-term PU: NH inp b (19), $-CN$ s (10), $-CH_\alpha^b$ inp b (5), CH_3^b asym def′ (4), $-CO$ inp b (2), $-CH_3$ asym def′ (2), $C_\alpha C$ s (1), CO s (1)
		C-term PU: N^aH^a inp b (26), $-C^aN^a$ s (12), $N^aC_\alpha^b$ s (4), $-C^aH_\alpha^a$ inp b (2), NC_α^a s (3), $-C^aO^a$ inp b (2), $C^aC_\alpha^a$ s (1), $-CH_3^b$ asym def (1), CH_3^b rocking′ (1)
	1495	N-term PU: NH inp b (28), $-CN$ s (15), CO inp b (3), $C_\alpha C$ s (2), $-CH_3$ asym def′ (1)
		C-term PU: N^aH^a inp b (20), C^aN^a s (8), NC_α^a s (4), CH_α^a inp b (4), $-N^aC_\alpha^b$ s (3), CH_3^a asym def′ (2), $-CH_\alpha^a$ inp b (2), C^aO^a inp b (1), $-C^aC_\alpha^a$ s (1), $-CH_3^b$ asym def′ (1), $-C^aO^a$ s (1)
PPII	1491	N-term PU: NH inp b (39), $-CN$ s (23), $C_\alpha C$ s (4), $-CO$ inp b (4), $-CH_3$ asym def′ (2), CH_α inp b (1), CO s (1), $-NH_2$ rocking (1)
		C-term PU: N^aH^a inp b (5), NC_α^a s (5), $-CH_\alpha^a$ inp b (4), $-C^aN^a$ s (3), CH_3^a asym def′ (2), $NC_\beta^aC_\alpha^a$ b (1), $N^aC_\alpha^b$ s(1)
	1495	C-term PU: N^aH^a inp b (44), $-C^aN^a$ s (25), $N^aC_\alpha^b$ s (6), $-N^aC_\alpha^b$ s (4), $C^aC_\alpha^a$ s (4), $-CH_3^a$ asym def′ (2), $C_\alpha^aH_\alpha^a$ inp b (2), $-C_\alpha^bH_\alpha^b$ inp b (1), $-NC_\alpha^a$ s (1), $N^aC_\beta^bC_\alpha^b$ b (1), CH_3^b asym def′ (1), $C_\alpha^bH_\alpha^b$ outp b (1), $-N^aC_pC_\alpha^b$ b (1)
		N-term PU: $-NH$ inp b (3), CN s (2)

[a] Frequencies are scaled by factor 0.97. Abbreviations: PU, peptide unit; s, stretch; b, bending; inp b, in-plane bending; outp b, out-of-plane bending; scs, scissoring.

TABLE 3: Calculated $AmIII_3$ Frequencies and Normal Mode Compositions of Trialanine[a]

conformer	ν, cm^{-1}	PED, %
α-helix	1222	C-term PU: C^aN^a s (18), N^aH^a inp b (17), $-C^aC_\alpha^a$ s (16), C^aO^a inp b (7), $-CH_\alpha^b$ outp b (6), $-N^aC_\alpha^b$ s (6), $C_\alpha^bH_\alpha^b$ inp b (4), NC_α^a s (3), CH_3^b rocking (2), $-NC_\beta^aC_\alpha^a$ b (2), CH_3^a rocking′ (2), $C^aNC_\alpha^a$ b (2), $-CH_3^a$ rocking (1), $C^aC_\beta^aC_\alpha^a$ b (1), $-CH_3^a$ asym def′ (1), CH_3^b rocking′ (1), CH_3^b asym def (1), $N^aC_pC_\alpha^b$ b (1), $-C_\alpha^aH_\alpha^a$ outp b (1), $N^aC_\beta^bC_\alpha^b$ b (1), $C_\alpha^aC_\beta^a$ s (1)
		N-term PU: $-NH_2$ rocking (2), $C_\alpha H_\alpha$ outp b (1), $-CO_p$ inp b (1)
	1247	N-term PU: NH inp b (17), CN s (10), $-NH_2$ rocking (12), CH_α outp b (10), $-C_\alpha C$ s (8), CO inp b (4), $-CH_3$ rocking (2), $-C_\beta N_pC_\alpha$ b (2), CO s (2), CH_3^a rocking (1), CN_pC_α b (1), $C_\alpha C_\beta$ s (1), CH_α inp b (1), $-CH_3$ asym def′ (1)
		C-term PU: $-C_\alpha^aH_\alpha^a$ outp b (12), $C_\alpha^aH_\alpha^a$ inp b (6), $C_\alpha^bH_\alpha^b$ outp b (2), $-NC_\alpha^a$ s (1), $-N^aH^a$ inp b (1), CH_3^a rocking′ (1), $-C^aN^a$ s (1), $-CH_\alpha^b$ inp b (1), CH_3^a asym def (1)
PPII	1205	C-term PU: C^aN^a s (21), N^aH^a inp b (16), $-N^aC_\alpha^b$ s (14), $N^aC_\alpha^b$ s (6), OH_{p*} inp b (6), $C_\alpha^aH_\alpha^a$ outp b (6), $C_\alpha^aH_\alpha^a$ inp b (5), CH_3^b rocking (4), $-C_\alpha^bH_\alpha^b$ outp b (4), $-C^aC_\alpha^a$ s (2), $N^aC_\beta^bC_\alpha^b$ b (1), $-CH_3^a$ rocking′ (1), $-C^aNC_\alpha^a$ b (1), $-CN_pC_\alpha$ b (1), $N^aC_pC_\alpha^b$ b (1), $-COp$ inp b (1), CN s (1), $C^aC_\alpha^bN^a$ b (1), $C_\alpha^bC_p$ s (1)
		N-term PU: $-NH_2$ rocking (3), NH inp b (1), N_pC_α s (1)
	1227	N-term PU: NH_2 rocking (18), $-CN$ s (16), $-NH$ inp b (13), $-CO$ inp b (7), CN_pC_α b (6), $-N_pC_\alpha$ s (3), $-C_\alpha H_\alpha$ outp b (3), $C_\alpha C$ s (2), $-CC_\beta C_\alpha$ b (2), $-CO$ s (1), CH_3 rocking′ (1), CH_3 rocking (1), $C_\beta N_pC_\alpha$ b (1), CH_3 asym def (1)
		C-term PU: $C_\alpha^aH_\alpha^a$ outp b (10), $N_\alpha^aC_\alpha^a$ s (5), $-C_\alpha^aH_\alpha^a$ inp b (2), $-CH_3^a$ rocking (2), $-CH_3^a$ rocking′ (1), $-CH_3^a$ asym def (1), $N^aC_\alpha^b$ s (1), $-C^aNC_\alpha^a$ b (1), N^aH^a inp b (1)

[a] Frequencies are scaled by factor 0.97. Abbreviations: PU, peptide unit; s, stretch; b, bending; inp b, in-plane bending; outp b, out-of-plane bending; scs, scissoring. $-NH_2$ rocking is a penultimate group vibration contribution.

overlap of HOD bending and arginine side-chain bands and the molecular O_2 stretching vibrations, which shows spectral intensity variations.[37]

Table 2 indicates two different amide II modes for the α-helical Ala_3 conformation (1480 and 1495 cm^{-1}), which derive from the in- and out-of-phase coupled vibrations of both peptide units. These amide II vibrations contain similar contributions of C−N stretching and N−H bending of both peptide units. For example, the 1495 cm^{-1} amide II vibration contains 28% N−H bending of the N-terminal peptide units and 20% N−H bending of the C-terminal peptide unit. In contrast, the two amide II vibrations of Ala_3 in the PPII conformation occur much closer in frequency and are almost local modes (Table 2).

Amide III_3. The amide III spectral region shows several bands that originate from vibrations involving C−N, N−C_α, C_α−C, and C−C_α stretching and N−H and C_α−H bending motions.[51] The “classic” amide III band (specifically the amide III_3) involves CN stretching with in-phase N−H bending, which couples to $C_\alpha H$ in-phase bending in the PPII conformation. This conformation-dependent coupling makes this amide III_3 band extremely sensitive to peptide secondary structure.[35] In the α-helical AP, this band occurs at 1261 cm^{-1}, and in the PPII conformation, the amide III_3 band occurs at 1245 cm^{-1}. The D_2O decoupling of ND bending from CN stretching and $C_\alpha H$ bending upon deuteration results in the disappearance of the amide III_3 band, as well as the other amide III region bands.[49,51,52] Our UVRS comparison between the α-helical and PPII bands of AP spectra in H_2O/D_2O mixtures indicated that the spectra could be modeled as the sum of the deuterated and protonated species in both the α-helical and PPII conformations. We concluded that there was insignificant coupling between the amide III_3 vibrations of adjacent peptide units.[37]

The conclusions from our theoretical studies are confounded by the fact that the two amide III_3 vibrations in Ala_3 differ significantly because the N-terminal peptide unit amide III_3 vibration selectively couples to the penultimate NH_2 rocking motion (Table 3). The amide III_3 vibration is very complicated. In addition to the atomic motions listed above, the amide III_3 vibration also has contributions from C_α−C stretching, CH_3 rocking (from the Ala methyl side-chain), and C=O in-plane bending. However, the main contributions are still from C−N

TABLE 4: Calculated Amide III_3 Frequencies and Normal Mode Compositions of ND_2-Substituted Ala_3[a]

conformer	ν, cm^{-1}	PED, %
α-helix	1218	C-term PU: C^aN^a s (14), N^aH^a inp b (12), $-C^aC_\alpha^a$ s (11), C^aO^a inp b (6), $-N^aC_\alpha^b$ s (4), $-C_\alpha^bH_\alpha^b$ outp b (4), $-C_\alpha^aH_\alpha^a$ outp b (4), $C_\alpha^bH_\alpha^b$ inp b (3), CH_3^a rock′ (3), $C^aNC_\alpha^a$ b (2), CH_3^b rock (1), $C^aC_\beta^aC_\alpha^a$ b (1), $-NC_\beta^aC_\alpha^a$ b (1), $-CH_3^a$ asym def′ (1), CH_3^b rock′ (1), NC_α^a s (1), CH_3^b asym def (1), $C_\alpha^aH_\alpha^a$ inp b (1)
		N-term PU: NH inp b (8), CN s (5), $-C_\alpha C$ s (5), $-NH_2$ scs (3), CO inp b (2), CO s (1), CN_pC_α b (1)
	1232	N-term PU: NH inp b (15), CN s (13), $-C_\alpha C$ s (10), CO inp b (5), CN_pC_α b (2), $-NH_2$ scs (1), CH_3 rock′ (1), $-NH_2$ rock (1), $-C_\beta N_pC_\alpha$ b (1), CO s (1), $-CH_3$ rock (1), $C_\alpha C_\beta$ s (1), $CC_\beta C_\alpha$ b (1), $-CH_3$ asym def′ (1)
		C-term PU: $-N^aH^a$ inp b (6), $-C^aN^a$ s (5), $C^aC_\alpha^a$s (5), $-C_\alpha^aH_\alpha^a$ outp b (5), $-NC_\alpha^a$ s (4), $C_\alpha^aH_\alpha^a$ inp b (4), $C_\alpha^bH_\alpha^b$ outp b (4), CH_3^a rock (2), $N^aC_\alpha^b$s (2), $-C_\alpha^bH_\alpha^b$ inp b (2), $-C^aO^a$ inp b (2), $NC_\beta^aC_\alpha^a$ b (1), $-CH_3^b$ rock (1), $-CH_3^b$ rock′ (1)
PPII	1201	C-term PU: $N^aC_{\alpha.}^b$ s (13), $-C^aN^a$ s (13), $-N^aH^a$ inp b (8), NC_α^a s (6), $-O_pH_{p*}$ inp b (5), $-CH_3^b$ rock (3), $-CH_\alpha^b$ inp b (3), $-C^aO^a$ inp b (2), $-CH_3^a$ rock (2), $C_\alpha^bH_\alpha^b$ outp b (2), $-N^aC_\beta^bC_\alpha^b$ b (1), $-NC_\beta^aC_\alpha^a$ b (1), $-C_\alpha^aN^aC^a$ b (1), $-C_\alpha^bC_p$ s (1), $-C^aC_\alpha^bN^a$ b (1), $-N^aC_pC_{\alpha.}^b$ b (1), $C_{p.}C\,_\beta^b\,C_\alpha^b$ b (1)
		N-terminal PU: $-CN$ s (11), $-NH$ inp b (8), $-C_\alpha H_\alpha$ inp b (4), $-CO$ inp b (4), $-C_\alpha H_\alpha$ outp b (1), CN_pC_α b (1), $-NH_2$ scs (1), $C_\alpha C$ s (1), NH_2 rock (1), CH_3 rock′ (1)
	1212	N-terminal PU: $-CN$ s (12), $-NH$ inp b (7), $-CO$ inp b (4), $-C_\alpha H_\alpha$ inp b (4), $-C_\alpha H_\alpha$ outp b (2), CN_pC_α b (1), $-CH_3^a$ asym def (1), CH_3 rock′ (1), $C_\alpha C$ s (1), NH_2 rock (1)
		C-terminal PU: C^aN^a s (9), N^aH^a inp b (9), CH_α^a outp b (13), NC_α^a s (9), C^aO^a inp b (4), $-CH_3^a$ rock (3), $-N^aC_\alpha^b$ s (3), $-C_\alpha^bH_\alpha^b$ outp b (3), $-C^aNC_\alpha^a$ b (2), $-CH_3^a$ rock′ (2), $-C^aC_\alpha^a$ s (2), OH_{p*} inp b (2), CH_3^b rock (1), $-NC_\beta^aC_\alpha^a$ b (1)

[a] Frequencies are scaled by factor 0.97. Abbreviations: PU, peptide unit; s, stretch; b, bending; inp b, in-plane; outp b, out-of-plane bending; scs, scissoring.

stretching and N−H bending. The amide III_3 normal modes in both the α-helix and PPII conformations of Ala_3 act as local modes in terms of contributions from C−N stretching and N−H bending from individual peptide units (Table 3).

The two amide III_3 bands in the α-helical conformation were calculated to occur at 1222 and 1247 cm^{-1}, with the 25 cm^{-1} higher frequency band corresponding to the vibration of the N-terminus peptide unit with contributions from the terminal NH_2 group rocking bending. A similar gap between two amide III_3 frequencies was calculated for the PPII conformation where the N-terminal peptide unit vibration also has a contribution from NH_2 rocking.

Because these two amide III_3 vibrations differ due to the unique NH_2 rocking contribution from the N-terminal group, it is likely that this calculation may not be relevant to the amide III_3 bonds of the internal peptide unit of peptides, which cannot include NH_2 rocking. Thus, we attempted to examine amide III_3 normal modes in Ala_3 isotopomers, which were uncoupled to the terminal NH_2 group motions; we examined the ND_2-deuterated derivative of Ala_3.

ND_2-deuteration decreases the frequency difference between the two amide III_3 bands to 14 cm^{-1} in the α-helical conformation and to 11 cm^{-1} in the PPII conformation (Table 4). In the ND_2 α-helical Ala_3 derivative, the higher frequency amide III_3 vibration is dominated by the N-terminus peptide unit but also contains a smaller contribution of motion from the other peptide unit. The low frequency amide III_3 band corresponds mainly to a C-terminus amide III_3 vibration with significant but smaller N−H bending and C−N stretching contributions from the other peptide unit.

The amide III_3 vibrations (1201 and 1212 cm^{-1}) in the PPII conformation of ND_2 Ala_3 are evidently coupled; both amide III_3 vibrations involve comparable contributions of CN stretching and NH bending from each peptide unit (Table 4). Our experimental results concluded little coupling evidenced by insignificant spectral frequency shifts upon deuteration of adjacent peptide units.

Frequency Shifts of the Amide Bands Due to Coupling. The coupling between local motions is monitored by the value of the coupling force constants, i.e., the off-diagonal elements of the Hessian matrix. For a system with two peptide bonds, the Hessian matrix is

$$\tilde{F}(\phi,\varphi) = \begin{bmatrix} K_1(\phi,\varphi) & C_{12}(\phi,\varphi) \\ C_{12}(\phi,\varphi) & K_2(\phi,\varphi) \end{bmatrix}$$

where K_1 and K_2 are force constants of the local modes and C_{12} is the coupling force constant between local modes.

Due to the nonzero coupling force constants, interaction between two local modes results in formation of two coupled delocalized modes with perturbed frequencies. In the case of amide I local mode coupling, two coupled amide I modes of symmetry A and E_1 are formed. The frequencies of the A and E_1 modes will occur at higher and lower frequencies relative to that of the unperturbed local C═O stretches. The A component refers to the symmetrical, in-phase stretching of C═O bonds. The E_1 component originates from asymmetric or out-of-phase stretching motions of C═O bonds. When the transition dipole moments of the C═O stretch are perpendicular to the axis of the peptide backbone (as in the PPII or β-strand-like conformations), the E_1 component will show strong IR absorbance and the A component will be active in Raman but vanish in IR measurements. For these conformations, there is a difference between the amide I frequency observable in IR and the amide I frequency observable in Raman. This frequency difference corresponds to the A−E_1 splitting, which originates from coupling of the local C═O stretches. By contrast, in the α-helix conformation, where the transition dipole moment of each peptide group is almost parallel to the helix axis, the A component acquires a strong IR absorbance in addition to Raman intensity. Therefore, α-helical peptides show an amide I band of A symmetry, which is observable in both the IR and Raman spectra; there will be no frequency difference between the IR and Raman observed amide I bands in this case. There are few published studies dedicated to the peptide secondary structure determination from experimentally measured A−E_1 splitting between the amide I Raman and IR frequencies.[25,53,54]

The frequency difference between coupled vibrations depends upon the magnitude of the vibrational coupling constant. The larger the coupling constant, the stronger the coupling and the

TABLE 5: Calculated Amide I Frequencies ($\mathrm{cm^{-1}}$) of Normal Abundance $\mathrm{Ala_3}$ and $\mathrm{Ala_3}$ Isotopomers in α-Helical and PPII Conformations

	α-helix	PPII
$\mathrm{C^{13}O^{18}{-}Ala_3}$ 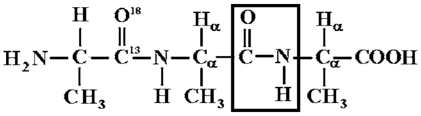	1712[a] l(C=O) = 1.224 Å	1699 l(C=O) = 1.229 Å
$\mathrm{C^{13}O^{18}{-}Ala_3}$ 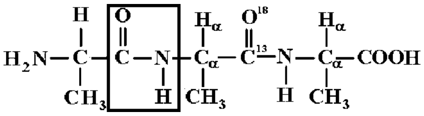	1708 l(C=O) = 1.226 Å	1695 l(C=O) = 1.231 Å
$\mathrm{Ala_3}$	1716 (A) 1702 ($\mathrm{E_1}$)	1698 (C term. PB) 1695 (N term. PB)

[a] Frequencies and C=O bond lengths correspond to indicated PB.

TABLE 6: Normal Mode Compositions of Amide I Vibrations of $\mathrm{D_2N}$, ND-Isotopomers of $\mathrm{Ala_3}$[a]

	PU deuterated	ν, $\mathrm{cm^{-1}}$	PED, %
α-helix	N-terminus	1715	C-term PU: $\mathrm{C^aO^a}$ s (60), $\mathrm{C_\alpha^aN^aC^a}$ b (5), $-\mathrm{C^aN^a}$ s (4), $-\mathrm{C^aC_\alpha^a}$ s (2), $-\mathrm{N^aH^a}$ inp b (2), $\mathrm{C^aC_\alpha^bN^b}$ b (1), $-\mathrm{C^aNC_\alpha^a}$ b (1) N-term PU: CO s (19), −CN s (2), $\mathrm{NC_\alpha C}$ b (2), $-\mathrm{C_\alpha C}$ s (1)
		1699	N-term PU: CO s (60), −CN s (5), $\mathrm{NC_\alpha C}$ b (5), $-\mathrm{C_\alpha C}$ s (2), $-\mathrm{CN_pC_\alpha}$ b (1) C-term PU: $-\mathrm{C^aO^a}$ s (19), $-\mathrm{C_\alpha^aN^aC^a}$ b (2), $\mathrm{C^aN^a}$ s (2), $\mathrm{C_\alpha^aCN}$ b (1), $\mathrm{C^aC_\alpha^a}$ s (1)
	C-terminus	1713	C-term PU: $\mathrm{C^aO^a}$ s (43), $\mathrm{C_\alpha^aN^aC^a}$ b (3), $-\mathrm{C^aN^a}$ s (3), $-\mathrm{C^aC_{\alpha.}^a}$ s (2) N-term PU: CO s (37), $\mathrm{NC_\alpha C}$ b (3), −CN s (3), $\mathrm{C_\alpha C}$ s (2)
		1701	N-term PU: CO s (41), $\mathrm{NC_\alpha C}$ b (4), −CN s (3), $-\mathrm{C_\alpha C}$ s (2), −NH inp b (1), $-\mathrm{CN_pC_\alpha}$ b (1) C-term PU: $-\mathrm{C^aO^a}$ s (37), $\mathrm{C^aN^a}$ s (3), $-\mathrm{C_\alpha^aN^aC^a}$ b (3), $\mathrm{C^aC_\alpha^a}$ s (1), $-\mathrm{C^aC_\alpha^bN^a}$ b (1), $\mathrm{C^aNC_\alpha{}^a}$ b (1), $\mathrm{C_\alpha^aCN}$ b (1)
PPII	N-terminus	1695	C-term PU: $\mathrm{C^aO^a}$ s (76), $-\mathrm{C^aN^a}$ s (8), $\mathrm{C_\alpha^aN^aC^a}$ b (6), $-\mathrm{C^aC_\alpha^a}$ s (2), $\mathrm{N^aC^aC_\alpha^b}$ b (2), $\mathrm{C^aNC_\alpha^a}$ b (1) N-term PU: CO s (3)
		1690	N-term PU: CO s (75), $\mathrm{NC_\alpha C}$ b (7), −CN s (6), $-\mathrm{C_\alpha C}$ s (3), −ND inp b (2), $\mathrm{CN_pC_\alpha}$ b (1) C-term PU: $-\mathrm{C^aO^a}$ s (3), $\mathrm{C_\alpha^aCN}$ b (2)
	C-terminus	1699	C-term PU: $\mathrm{C^aO^a}$ s (78), $-\mathrm{C^aN^a}$ s (7), $\mathrm{C_\alpha^aN^aC^a}$ b (7), $-\mathrm{C^aC_\alpha^a}$ s (3), $-\mathrm{N^aD^a}$ inp b (2), $\mathrm{C^aC_\alpha^bN^a}$ b (2), $\mathrm{C^aNC_\alpha^a}$ b (1)
		1685	N-term PU: CO s (79), −CN s (7), $\mathrm{NC_\alpha C}$ b (7), $-\mathrm{C_\alpha C}$ s (3), $\mathrm{CN_pC_\alpha}$ b (1), −NH inp b (1) C-term PU: $\mathrm{C_\alpha^aCN}$ b (2)

[a] Frequencies are scaled by factor 0.97. Abbreviations: PU, peptide unit; s, stretch; b, bending; inp b, in-plane; outp b, out-of-plane bending; scs, scissoring.

more the frequencies of coupled bands are perturbed compared to the frequencies of the local uncoupled bands. Therefore, we can estimate the strength of the amide band coupling by monitoring the frequency differences between calculated amide bands compared to the frequencies of the original uncoupled local vibrations. To obtain these uncoupled frequencies, we calculated the normal modes of various $\mathrm{Ala_3}$ isotopomers.

Amide I. The PED of the α-helical natural abundance $\mathrm{Ala_3}$ normal modes shows that the two calculated amide I bands (1702 and 1716 $\mathrm{cm^{-1}}$) are coupled modes of A and $\mathrm{E_1}$ symmetry. We singly substituted $\mathrm{C^{13}{-}O^{18}}$ at each of the two $\mathrm{Ala_3}$ peptide bonds and calculated the frequency of the other natural abundance peptide bond. In this case, the local amide I vibrations at the carboxyl end occurred at 1712 $\mathrm{cm^{-1}}$ and at the amine end occurred at 1708 $\mathrm{cm^{-1}}$. The frequencies differ because their optimized structures have slightly different C=O bond lengths (Table 5). If we assume a reference frequency for the uncoupled local C=O stretching mode of $\mathrm{Ala_3}$ as a simple average (1710 $\mathrm{cm^{-1}}$) of the local amide I frequencies calculated for two $\mathrm{Ala_3}$ isotopomers, we conclude that the coupling interactions in natural abundance $\mathrm{Ala_3}$ up-shift the high frequency A component by 6 $\mathrm{cm^{-1}}$ and down-shifts the $\mathrm{E_1}$ component by 8 $\mathrm{cm^{-1}}$ (Tables 5 and 10). In contrast, the PPII $\mathrm{Ala_3}$ PED shows that two calculated amide I modes are uncoupled and their frequencies are almost equal to the uncoupled amide I frequencies of $\mathrm{Ala_3}$ isotopomers. These results are fully consistent with our experimental data. Our results are also consistent with Torii and Tasumi[17] who theoretically showed that the coupling constants between adjacent amide I vibrations in the α-helix conformation are larger than those in the β-region (close to that of PPII conformation).

There are two main mechanisms of vibrational coupling: through bond coupling (or mechanical coupling) and through space coupling (or electrostatic coupling). Mechanical coupling results from the impact of local atomic motion on the structure of adjacent molecular bonds; electrostatic coupling results from the motion of local dipolar bonds. The large dipole moment of the C−O bond gives rise to significant electrostatic coupling for the amide I modes in addition to significant mechanical coupling. In contrast, mechanical coupling dominates the coupling between the amide II and amide $\mathrm{III_3}$ vibrations due to the smaller dipole moments of the vibrating bonds.

Amide I coupling in the α-helix conformation and the lack of it in the PPII conformation result from the different relative spatial orientations of the C=O bonds in the α-helix and PPII conformations.

In the α-helix, the C=O bonds are almost co-parallel; in the PPII conformation, they project out at angles of ∼120° from one another. The more they project upon one another, the larger

TABLE 7: Calculated Amide I, Amide II, and Amide III$_3$ Frequencies of Normal Abundance Ala$_3$ and Ala$_3$ Isotopomers in PPII and α-Helical Conformations

		amide I		amide II		amide III$_3$	
deuteration	conform	N-term.	C-term.	N-term.	C-term.	N-term.	C-term.
none	α-helix	1702 out-of-phase 1716 in-phase		1480 in-phase 1495 out-of-phase		1247	1222
	PPII	1695	1698	1491	1495	1227	1205
ND$_2$	α-helix	1702 out-of-phase 1716 in-phase		1480 in-phase 1496 out-of-phase		1232	1218
	PPII	1691	1699	1491	1496	1201 in-phase 1212 out-of-phase	
ND−N term	α-helix	1699 out-of-phase 1715 in-phase		ND	1487	ND	1221
	PPII	1690	1699	ND	1495	ND	1206
ND−C term	α-helix	1701 out-of-phase 1713 in phase		1489	ND	1245	ND
	PPII	1694	1695	1492	ND	1226	ND
ND$_2$, ND−N term	α-helix	1699 out-of-phase 1715 in-phase		ND	1487	ND	1221
	PPII	1685	1699	ND	1495	ND	1206
ND$_2$, ND−C term	α-helix	1701 out-of-phase 1713 in-phase		1489	ND	1227	ND
	PPII	1690	1695	1491	ND	1207	ND

TABLE 8: Normal Mode Compositions of Amide II Vibrations of D$_2$N, ND-Isotopomers of Ala$_3$[a]

	deuterated PU	ν, cm^{-1} [a]	PED, %
α-helix	N-terminus	1487	C-term PU: N^aH^a inp b (47), $-C^aN^a$ s (20), $-C_\alpha^bH_\alpha^b$ inp b (9), $N^aC_\alpha b$ s (6), CH_3^b asym def′ (3), $-C^aO^a$ inp b (3), $C^aC_{\alpha.}^a$ s (2), $-CH_3^a$ asym def′ (2), $-CH_3^b$ asym def (1), CH_3^b rocking′ (1), C^aO^a s (1)
	C-terminus	1489	N-term PU: NH inp b (47), −CN s (25), −CO inp b (4), $-C_\alpha C$ s (3), $-CH_3$ asym def′ (2), CO s (1) C-term PU: NC_α^a s (7), $C_\alpha^aH_\alpha^a$ inp b (4), CH_3^a asym def′ (2), $C_\alpha^aH_\alpha^a$ outp b (1), $NC_\beta^aC_\alpha^a$ b (1)
PPII	N-terminus	1495	C-term PU: N^aH^a inp b (49), $-C^aN^a$ s (28), $N^aC_{\alpha.}^b$ s (7), $-C^aO^a$ inp b (5), $C^aC_\alpha^a$ s (4), $-C_\alpha^bH_\alpha^b$ inp b (1), $N^aC_\beta^bC_\alpha^b$ b (1), $-CH_3^a$ asym def′ (1), CH_3^b asym def′ (1), $C_\alpha^bH_\alpha^b$ outp b (1), $C_\alpha^aH_\alpha^a$ inp b (1), $-N^aC_pC_\alpha^b$ b (1)
	C-terminus	1491	N-term PU: NH inp b (43), −CN s (25), −CO inp b (4), $C_\alpha C$ s (4), −CH3 asym def′ (1), CO s (1), $C_\alpha H_\alpha$ inp b (1) C-term PU: NC_α^a s (6), $-C_\alpha^aH_\alpha^a$ inp b (6), CH_3^a asym def′ (3), $NC_\beta^aC_\alpha^a$ b (1), $-CH_3^a$ asym def (1)

[a] Frequencies are scaled by factor 0.97. Abbreviations: PU, peptide unit; s, stretch, b, bending; inp b, in-plane; outp b, out-of-plane bending; scs, scissoring.

TABLE 9: Normal Mode Compositions of Localized Amide III$_3$ Vibrations of D$_2$N, ND-Isotopomers of Ala$_3$[a]

	deuterated PU	ν, cm^{-1} [a]	PED, %
α-helix	N-terminus	1221	C-term PU: C^aN^a s (19), N^aH^a inp b (18), $-C^aC_\alpha^a$ s (16), C^aO^a inp b (8), $-C_\alpha^bH_\alpha^b$ outp b (7), $-N^aC_\alpha^b$ s (6), $C_\alpha^bH_\alpha^b$ inp b (4), CH_3^b rock (2), $-NC_\beta^aC_\alpha^a$ b (2), $C^aNC_\alpha^a$ b (2), NC_α^a s (2), $-CH_3^a$ rock (2), CH_3^a rock′ (2), $-CH_3^a$ asym def′ (1), CH_3^a asym def′ (1), CH_3^b rock′ (1), CH_3^b asym def (1), $N^aC_pC_\alpha^b$ b (1), $C_\alpha^aC_\beta^a$ s (1), $N^aC_\beta^bC_\alpha^b$ b (1), $-C_pO_p$ inp b (1), $C^aC_\alpha^bN^a$ b (1)
	C-terminus	1227	N-term PU: NH inp b (24), CN s (19), $-C_\alpha C$ s (16), −CO inp b (8), CN_pC_α b (3), $-ND_2$ sciss (2), −CO s (1), CH_3 rock′ (1), $-ND_2$ rock (1), $C_\alpha C_\beta$ s (1), $-C_\beta N_pC_\alpha$ b (1), $-CH_3$ rock (1), $CC_\beta C_\alpha$ b (1), $-CH_3$ asym def′ (1) C-term PU: $C_\alpha^aH_\alpha^a$ outp b (10), NC_α^a s (2), $C_\alpha^aH_\alpha^a$ inp b (4), CH_3^a rock′ (1), CH_3^a rock (1), CH_3^a asym def (1)
PPII	N-terminus	1206	C-term PU: C^aN^a s (23), N^aH^a inp b (17), $-N^aC_\alpha^b$ s (13), $C_\alpha^aH_\alpha^a$ outp b (10), C^aO^a inp b (7), OH_{p*} inp b (6), $-C_\alpha^bH_\alpha^b$ outp b (4), CH_3^b rock (4), $C_\alpha^aH_\alpha^a$ inp b (3), $-CH_3^a$ rock′ (2), $-C^aC_\alpha^a$ s (2), $-C^aNC_\alpha^a$ b (1), $N^aC_\beta^bC_\alpha^b$ b (1), $N^aC_pC_\alpha^b$ b (1), $-C_pO_p$ inp b (1) N-term PU: $NC_\alpha C$ b (1)
	C-terminus	1207	N-term PU: CN s (24), NH inp b (14), CO inp b (8), $C_\alpha H_\alpha$ inp b (7), $C_\alpha H_\alpha$ outp b (4), $-CN_pC_\alpha$ b (2), $-C_\alpha C$ s (1), $-CH_3$ rock′ (1), $-ND_2$ rock (1) C-term PU: $-NC_\alpha^a$ s (16), CH_3^a rock (5), $-C_\alpha^aH_\alpha^a$ outp b (4), $NC_\beta^aC_\alpha^a$ b (2), $-N^aC_\alpha^a$ s (1), $C_\alpha^aN^aC^a$ b (1), C_α^a CN b (1), $C^aNC_\alpha^a$ b (1), CH_3^a asym def (1), $C_\alpha^aH_\alpha^a$ inp b (1), $C^aC_\alpha^a$ s (1), CH_3^a rock′ (1)

[a] Frequencies are scaled by factor 0.97. Abbreviations: PU, peptide unit; s, stretch; b, bending; inp b, in-plane; outp b, out-of-plane bending; scs, scissoring.

will be the dipole−dipole interactions. In addition, the closer the distance between C═O bonds, the stronger the dipole−dipole interactions. An α-helix conformation has a smaller pitch than the more extended PPII structure; the C═O and N−H bonds of neighboring peptide bonds are closer to each other compared to PPII or β-strand conformations.

Deuteration of the peptide bond NH and penultimate amino group does not affect the coupled amide I frequencies and

TABLE 10: Vibrational Coupling Frequency Shifts of Amide Bands

conformation		$\Delta\nu_{\text{amide I}}$, cm^{-1}	$\Delta\nu_{\text{amide II}}$, cm^{-1}	$\Delta\nu_{\text{amide III}_3}$, cm^{-1}
α-helix	in-phase	6	8	−3
	out-of-phase	−8	−8	5
PPII	in-phase	no coupling	no coupling	−5
	out-of-phase	occurs	occurs	6

TABLE 11: Measured PPII AP Frequencies, Calculated Frequencies of PPII Ala$_3$ in Vacuum and in Ala$_3$−Water Complex, and Calculated Hydrogen-Bonding Frequency Shifts

	$\nu_{\text{amide I}}$, cm^{-1}	$\nu_{\text{amide II}}$, cm^{-1}	$\nu_{\text{amide III}}$, cm^{-1}
ala$_3$ vacuum	1699	1496	1205
ala$_3$·4H$_2$O	1657	1559	1249
$\Delta\nu_{\text{HB}}$[a]	−42	63	44
PPII AP	1660	1558	1248

[a] $\Delta\nu_{\text{HB}} = \nu_{\text{Ala3}\times\text{4W}} - \nu_{\text{Ala3 gas}}$.

normal mode compositions in the α-helical conformation compared to the amide I frequencies of normal abundance Ala$_3$. In the PPII conformation, the amide I frequencies slightly shift upon deuteration (Tables 6 and 7). In the normal abundance PPII Ala$_3$ conformation, these modes are mainly C=O stretching vibrations of each individual peptide unit containing minor contributions (2%) from N−H bending. In addition to the N−H bending, the local amide I vibration of the N-terminal peptide unit has a contribution from NH$_2$ scissoring (4%) (Table 1). Deuteration of the NH$_2$ group or N−H bond eliminates contributions of N−H bending and NH$_2$ scissoring vibrations from the normal mode compositions, which results in slight frequency shifts (4−10 cm^{-1}) of the amide I frequencies (Table 7).

Amide II. No vibrational coupling occurs between amide II bands in the PPII conformation of Ala$_3$. These amide II frequencies are almost equal to the local frequencies (1496 and 1491 cm^{-1}) of isotopically substituted Ala$_3$ (Tables 7 and 8). The difference between two frequencies of regular Ala$_3$ (4 cm^{-1}) and two local frequencies of the Ala$_3$-isotopomers (5 cm^{-1}) originates from a slight difference between the C−N bond lengths of the two peptide bonds and is unrelated to any coupling.

We calculate that coupling between the amide II bands of α-helical Ala$_3$ results in formation of two delocalized vibrations which are up- and down-shifted by 8 cm^{-1} compared to the uncoupled localized amide II vibrations of the ND-substituted Ala$_3$ (Tables 7 and 10). However, for ND-deuterated α-helical Ala$_3$, we also calculate that the uncoupled amide II vibration should occur around 1487−1489 cm^{-1} (excluding frequency shift due to hydrogen bonding). This differs from the coupled amide II band frequencies calculated at 1480 and 1496 cm^{-1}.

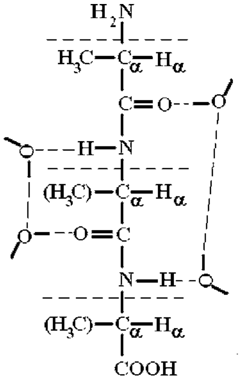

Figure 2. Water bridges in PPII structure.

These results indicate that we should observe more often the narrow amide II band in partially deuterated peptides than those fully protonated bands in pure water. It is possible that this shift was obscured by the overlap of the amide II band with an arginine band and the molecular oxygen stretching band.

Amide III$_3$. For α-helical NH$_2$, NH-deuterated Ala$_3$ isotopomers, our calculations show a 6 cm^{-1} frequency difference between local amide III$_3$ bands (1221 and 1227 cm^{-1}) of the N- and C-terminal peptide bonds.

In ND$_2$-substituted α-helical Ala$_3$, the amide III$_3$ vibrations are mainly localized. The higher frequency amide III$_3$ band (1232 cm^{-1}) is dominated by the motion of the N-terminal peptide unit with only a minor contribution from the C-terminal peptide unit (Table 4); the low frequency amide III$_3$ vibration (1218 cm^{-1}) contains a major contribution from the C-terminus peptide unit. The local amide III$_3$ vibrations of ND, ND$_2$-deuterated Ala$_3$ isotopomers occur at 1227 cm^{-1} (N-terminus vibration) and at 1221 cm^{-1} (C-terminus vibration) (Table 9). Vibrational coupling with the other peptide unit up-shifts this band by 5 cm^{-1}. Consequently, amide III$_3$ bands are 5 up- and 3 cm^{-1} down-shifted (Table 10). We conclude that α-helical amide III$_3$ band coupling is small because the frequencies shift little from the frequencies of local vibrations. However, the normal mode compositions of these two calculated amide III$_3$ vibrations indicate some contributions from the adjacent peptide unit.

The PPII conformation N- and C-terminus amide III$_3$ vibrations of the ND$_2$, ND-substituted Ala$_3$ isotopomers have almost identical frequencies (1206, 1207 cm^{-1}). Therefore, in natural abundance Ala$_3$, the symmetrical component (1201 cm^{-1}) of amide III$_3$ is down-shifted by 5 cm^{-1} and the asymmetrical

TABLE 12: Amide Frequencies of AP (Measured) and Ala$_3$ (Calculated) in PPII Conformation in Gas-Phase and in Peptide−Water Complex

	amide I, cm^{-1}		amide II, cm^{-1}		amide III$_3$, cm^{-1}	
	N-term.	C-term.	N-term.	C-term.	in-phase	out-of-phase
PPII−ala$_3$, calc	1690 (1648)	1699 (1657)	1491 (1554)	1496 (1558)	1201 (1245)	1212 (1256)
PPII−AP in H$_2$O, experimental	1660		1558		1245	
PPII−AP in H$_2$O/D$_2$O experimental	1655		1559		1248	
PPII−AP in H$_2$O/D$_2$O modeled spectra without coupling	1661		1560		1249	

[a] Values in parentheses include $\Delta\upsilon_{\text{HB}}$ (see Table 11).

TABLE 13: Measured Frequencies of Gas-Phase and Liquid NMA, Calculated Hydrogen-Bonding Frequency Shifts ($\Delta\nu_{HB}$), Calculated Frequencies of α-Helical Ala_3 in Vacuum, Frequencies of the α-Helical Ala_3 Including $\Delta\nu_{HB}$, and Measured Frequencies of α-Helical AP

	$\nu_{amide\ I}$, cm^{-1}	$\nu_{amide\ II}$, cm^{-1}	$\nu_{amide\ III3}$, cm^{-1}
NMA, gas phase[a] measured	1731	1499	1255
NMA, neat liquid measured	1668	1558	1298
$\Delta\nu_{HB}$[b]	−63	59	43
α-Ala_3, gas phase calcd	1702	1480	1218
α-Ala_3 + $\Delta\nu$	1639	1539	1261
α-AP, experimental	1646	1547	1261

[a] Kubelka, J.; Keiderling, T. *J. Phys. Chem. A* **2001**, 10922−10928. [b] $\Delta\nu_{HB} = \nu_{NMA\ liquid} - \nu_{NMA\ gas}$.

component (1212 cm^{-1}) is up-shifted by 6 cm^{-1} due to vibrational coupling (Tables 4 and 10). Our calculations show weak coupling of the PPII amide III_3 bands. This PPII amide III_3 coupling can be explained by its normal mode compositions. Besides the C−N stretch and N−H bending, which are coupled in-phase with C_α−H bending, the PPII amide III_3 modes contain contributions from the N−C_α stretching vibration (Table 4). The N−C_α bond "bridges" adjacent peptide units. This stretching motion facilitates coupling with the C_α−H bending motions. The C_α−H bending can efficiently couple with N−H bending of the adjacent peptide unit. The contribution from the N−C_α stretch facilitates delocalization of the PPII amide III_3 band. The amide III_3 vibration of α-helical Ala_3 does not include the N−C_α stretching. Instead, this normal mode contains C−C_α stretching.

Frequency Shifts of the Amide Bands Due to Hydrogen Bonding. Our calculated amide frequencies differ from the experimentally measured frequencies because we have not taken into account the effects of hydrogen bonding. The hydrogen-bonding patterns differ in the α-helix and PPII conformations. Hydrogen bonding in the PPII conformation involves hydrogen bonding to water. Hydrogen bonding in the α-helix conformation involves peptide bond−peptide bond hydrogen bonding.

Hydrogen-Bonding Shifts in PPII Conformation. To estimate the effects of the hydrogen-bonding differences on the frequencies of the amide vibrations we compared amide I, amide II, and amide III_3 frequencies calculated for the PPII Ala_3 in vacuum to the Ala_3−water complex.

Sreerama et al.[55] studied the network of water molecules involved in hydrogen bonding to the backbone of polyalanine in β-strand and PPII conformations by molecular dynamics simulations. They analyzed populations of different types of hydrogen-bonding "bridges". For the PPII conformation, they found that a bridge of two water molecules connecting the *i*-th C═O and (*i* + 2)-th N−H bonds was the most populated.

We calculated the frequencies of an Ala_3−water complex in the PPII conformation for this arrangement of water molecules (see Figure 2). We included four water molecules, which made two water bridges: one connects the first residue C═O bond with the third residue N−H bond and the other connects the remaining N−H and C═O groups in the second residue (Figure 2). This hydrogen-bonding network down-shifts the amide I frequency of Ala_3 by 42 cm^{-1} and up-shifts the amide II and amide III_3 bands by 63 and 44 cm^{-1}, respectively (Table 11). Overall, the amide frequencies calculated for the Ala_3−water complex agree well with the experimentally measured frequencies of PPII AP (Table 12).

Hydrogen-Bonding Shifts in α-Helical Conformation. Theoretical simulation of the intermolecular hydrogen bonding in the α-helix conformation is more complicated. We estimated the α-helix hydrogen-bonding frequency shifts from a difference between UVRR amide band frequencies of the gas phase[56] and liquid state[35] of *N*-methylacetamide (NMA) (Table 13). The frequency of the amide I band decreases by 63 cm^{-1} in liquid NMA, compared to the gas state, and the amide II and amide III_3 frequencies increase by ~60 and 43 cm^{-1}, respectively. We applied these frequency shifts to correct the calculated frequencies of vacuum α-ala_3. This correction brings calculated Ala_3 frequencies into a good agreement with the measured frequencies of α-helical AP (Table 14).

Conclusion

Our calculations have demonstrated vibrational coupling between adjacent peptide units of the amide I and amide II modes in the α-helical conformation where these carbonyl bonds are closest to each other and their projection angles are smallest. This coupling decreases in the PPII conformation, because the structure is more extended and the projection angle increases.

The favorable orientation of the C═O bonds in the α-helix conformation facilitates transitional dipole coupling. Therefore, coupling of the amide I bands is much larger than coupling between the amide II bands.

Coupling interactions between amide III_3 bands is less than that of the amide I and amide II vibrations. The amide III_3 bands can be treated as a local vibrations of independently Raman scattering peptide bonds. The calculated amide III_3 frequencies are not significantly perturbed compared to the frequencies of local amide III_3 modes even though our calculations indicate that their normal mode compositions contain minor contributions from the adjacent peptide units.

Acknowledgment. We gratefully acknowledge Alexander Mikhonin for useful discussions. This work was supported by NIH grant GM8RO1EB002053021.

TABLE 14: Measured and Calculated Frequencies of AP and Ala_3 in α-Helical Conformations[a]

	amide I, cm^{-1}		amide II, cm^{-1}		amide III_3, cm^{-1}	
	in-phase	out-of-phase	in-phase	out-of-phase	in-phase	out-of-phase
α-Ala_3, calcd	1716 (1653)	1702 (1639)	1480 (1539)	1496 (1555)	1218 (1261)	1232 (1275)
α-AP in H_2O, experimental	1646		1547		1261	
α-AP in H_2O/D_2O, experimental	1644		1535		1256	
α-AP in H_2O/D_2O modeled spectra without coupling	1643		1530		1262	

[a] Values in parenthesis include $\Delta\nu_{HB}$ (see Table 11).

References and Notes

(1) Choi, J.-H.; Hahn, S.; Cho, M. *Int. J. Quantum Chem.* **2005**, *104*, 616.

(2) Edler, J.; Hamm, P. *J. Chem. Phys.* **2002**, *117*, 2415.

(3) Fang, C.; Wang, J.; Charnley, A. K.; Barber-Armstrong, W.; Smith, A. B.; Decatur, S. M.; Hochstrasser, R. M. *Chem. Phys. Lett.* **2003**, *2003*, 586.

(4) Hamm, P.; Lim, M.; Hochstrasser, R. M. *J. Phys. Chem. B* **1998**, *102*, 6123.

(5) Fang, C.; Wang, J.; Kim, Y. S.; Charnley, A. K.; Barber-Armstrong, W.; Smith, A. B. I.; Decatur, S. M.; Hochstrasser, R. M. *J. Phys. Chem. B* **2004**, *108*, 10415.

(6) Bowen, M.; Brunger, A. T. *Proc. Natl. Acad. Sci. U.S.A.* **2006**, *103*, 8378.

(7) Ahmed-Ouameur, A.; Diamantoglou, S.; Sedaghat-Herati, M. R.; Nafisi, S.; Carpentier, R.; Tajmir-Riahi, H. A. *Cell Biochem. Biophys.* **2006**, *45*, 203.

(8) Perham, M.; Liao, J.; Wittung-Stafshede, P. *Biochemistry* **2006**, *45*, 7740.

(9) Xu, Y.; Wang, T.; Gai, F. *Chem. Phys.* **2006**, *323*, 21.

(10) Causgrove, T. P.; Dyer, R. B. *Chem. Phys.* **2006**, *323*, 2.

(11) Pozo Ramajo, A.; Petty, S. A.; Volk, M. *Chem. Phys.* **2006**, *323*, 11.

(12) Chin, W.; Piuzzi, F.; Dimicoli, I.; Mons, M. *Phys. Chem. Chem. Phys.* **2006**, *8*, 1033.

(13) Du, D.; Tucker, M. J.; Gai, F. *Biochemistry* **2006**, *45*, 2668.

(14) Decatur, S. M. *Acc. Chem. Res.* **2006**, *39*, 169.

(15) Manning, M. C. *Expert Rev. Proteomics* **2005**, *2*, 731.

(16) Gorbunov, R. D.; Kosov, D. S.; Stock, G. *J. Chem. Phys.* **2005**, *122*, 224904/1.

(17) Torii, H.; Tasumi, M. *J. Raman Spectrosc.* **1998**, *29*, 81.

(18) Choi, J.-H.; Ham, S.; Cho, M. *J. Chem. Phys.* **2002**, *117*, 6821.

(19) Ham, S.; Cho, M. *J. Chem. Phys.* **2003**, *118*, 6915.

(20) Ham, S.; Cha, S.; Choi, J.-H.; Cho, M. *J. Chem. Phys.* **2003**, *119*, 1451.

(21) Choi, J.-H.; Ham, S.; Cho, M. *J. Phys. Chem. B* **2003**, *107*, 9132.

(22) Ham, S.; Kim, J.-H.; Lee, H.; Cho, M. *J. Chem. Phys.* **2003**, *118*, 3491.

(23) Bour, P.; Keiderling, T. A. *J. Chem. Phys.* **2003**, *119*, 11253.

(24) Fang, C.; Wang, J.; Charnley, A. K.; Barber-Armstrong, W.; Smith, A. B.; Decatur, S. M.; Hochstrasser, R. M. *Chem. Phys. Lett.* **2003**, *382*, 586.

(25) Schweitzer-Stenner, R. *J. Phys. Chem. B* **2004**, *108*, 16965.

(26) Schweitzer-Stenner, R.; Sieler, G.; Mirkin, N. G.; Krimm, S. *J. Phys. Chem. A* **1998**, *102*, 118.

(27) Huang, Q.; Schweitzer-Stenner, R. *J. Raman Spectrosc.* **2004**, *35*, 586.

(28) Krimm, S.; Abe, Y. *Proc. Natl. Acad. Sci. U.S.A.* **1972**, *69*, 2788.

(29) Moore, W. H.; Krimm, S. *Proc. Natl. Acad. Sci. U.S.A.* **1975**, *72*, 4933.

(30) Cheam, T. C.; Krimm, S. *Chem. Phys. Lett.* **1984**, *107*, 613.

(31) Krimm, S.; Bandekar, J. *Adv. Protein Chem.* **1986**, *38*, 181.

(32) Torii, H.; Tatsumi, T.; Tasumi, M. *J. Raman Spectrosc.* **1998**, *29*, 537.

(33) Asher, S. A.; Ianoul, A.; Mix, G.; Boyden, M. N.; Karnoup, A.; Diem, M.; Schweitzer-Stenner, R. *J. Am. Chem. Soc.* **2001**, *123*, 11775.

(34) Ianoul, A.; Boyden, M. N.; Asher, S. A. *J. Am. Chem. Soc.* **2001**, *123*, 7433.

(35) Mikhonin Aleksandr, V.; Bykov Sergei, V.; Myshakina, Nataliya, S.; Asher, Sanford, A. *J. Phys. Chem. B* **2006**, *110*, 1928.

(36) Mix, G.; Schweitzer-Stenner, R.; Asher, S. A. *J. Am. Chem. Soc.* **2000**, *122*, 9028.

(37) Mikhonin, A. V.; Asher, S. A. *J. Phys. Chem. B* **2005**, *109*, 3047.

(38) Kohn, W.; Sham, L. J. *Phys. Rev.* **1965**, *137*, 1697.

(39) Parr, R. G.; W. Yang *Density-functional theory of atoms and molecules*; Oxford University Press: Oxford, U.K., 1989.

(40) Hohenberg, P.; Kohn, W. *Phys. Rev.* **1964**, *136*, B864.

(41) Frisch, M. J. T., G. W.; Schlegel, H. B.; Scuseria, G. E.; Robb, M. A.; Cheeseman, J. R.; Montgomery, Jr., J. A.; Vreven, T.; Kudin, K. N.; Burant, J. C.; Millam, J. M.; Iyengar, S. S.; Tomasi, J.; Barone, V.; Mennucci, B.; Cossi, M.; Scalmani, G.; Rega, N.; Petersson, G. A.; Nakatsuji, H.; Hada, M.; Ehara, M.; Toyota, K.; Fukuda, R.; Hasegawa, J.; Ishida, M.; Nakajima, T.; Honda, Y.; Kitao, O.; Nakai, H.; Klene, M.; Li, X.; Knox, J. E.; Hratchian, H. P.; Cross, J. B.; Bakken, V.; Adamo, C.; Jaramillo, J.; Gomperts, R.; Stratmann, R. E.; Yazyev, O.; Austin, A. J.; Cammi, R.; Pomelli, C.; Ochterski, J. W.; Ayala, P. Y.; Morokuma, K.; Voth, G. A.; Salvador, P.; Dannenberg, J. J.; Zakrzewski, V. G.; Dapprich, S.; Daniels, A. D.; Strain, M. C.; Farkas, O.; Malick, D. K.; Rabuck, A. D.; Raghavachari, K.; Foresman, J. B.; Ortiz, J. V.; Cui, Q.; Baboul, A. G.; Clifford, S.; Cioslowski, J.; Stefanov, B. B.; Liu, G.; Liashenko, A.; Piskorz, P.; Komaromi, I.; Martin, R. L.; Fox, D. J.; Keith, T.; Al-Laham, M. A.; Peng, C. Y.; Nanayakkara, A.; Challacombe, M.; Gill, P. M. W.; Johnson, B.; Chen, W.; Wong, M. W.; Gonzalez, C.; Pople, J. A. *Gaussian 03*; revision C.01; Gaussian, Inc.: Wallingford, CT, 2004.

(42) Becke, A. D. *J. Chem. Phys.* **1993**, *98*, 5648.

(43) Lee, C.; Yang, W.; Parr, R. G. *Phys. Rev. B: Condens. Matter Mater. Phys.* **1988**, *37*, 785.

(44) Miehlich, B.; Savin, A.; Stoll, H.; Preuss, H. *Chem. Phys. Lett.* **1989**, *157*, 200.

(45) Mu, Y.; Stock, G. *J. Phys. Chem. B* **2002**, *106*, 5294.

(46) Irikura, K. K.; Johnson, R. D., III;, Kacker, R. N. *J. Phys. Chem. A* **2005**, *109*, 8430.

(47) Halls, M. D.; Velkovski, J.; Schlegel, H. B. *Theor. Chem. Acc.* **2001**, *105*, 413.

(48) Martin, J. M. L.; Van Alsenoy, C. *GAR2PED*; University of Antwerpen: Antwerpen, Belgium, 1995.

(49) Lee, S.-H. K., S. *Biopolymers* **1998**, *46*, 283.

(50) Chen, X. G.; Asher, S. A.; Schweitzer-Stenner, R.; Mirkin, N. G.; Krimm, S. *J. Am. Chem. Soc.* **1995**, *117*, 2884.

(51) Mikhonin, A. V.; Ahmed, Z.; Ianoul, A.; Asher, S. A. *J. Phys. Chem. B* **2004**, *108*, 19020.

(52) Lednev, I. K. K., A. S.; Sparrow, M. C.; Asher, S. A. *J. Am. Chem. Soc.* **2001**, *1231*, 2388.

(53) Sugawara, Y.; Harada, I.; Matsuura, H.; Shimanouchi, T. *Biopolymers* **1978**, *17*, 1405.

(54) Painter, P. C.; Koenig, J. L. *Biopolymers* **1976**, *15*, 229.

(55) Sreerama, N.; Woody, R. W. *Proteins: Struct., Funct., Gen.* **1999**, *36*, 400.

(56) Kubelka, J.; Keiderling, T. A. *J. Phys. Chem. A* **2001**, *105*, 10922.